

# Ab Initio Diradical/Zwitterionic Polarizabilities and Hyperpolarizabilities in Twisted Double Bonds

Christine M. Isborn, Ernest R. Davidson, and Bruce H. Robinson\*

Department of Chemistry, University of Washington, Seattle, Washington 98195-1700

Received: November 14, 2005; In Final Form: March 2, 2006

We investigated the nature of the ground state and static response properties ( $\mu$ ,  $\alpha$ , and  $\beta$ ) for a promising class of twisted  $\pi$ -electron system nonlinear optical chromophores at the HF, B3LYP, MP2, and CASSCF levels. We report results for a substituted twisted ethylene and a larger tictoid analogue. Previous work has reported only a zwitterionic character for such tictoid species, however, (14,13) CASSCF calculations predict a ground-state diradical. At the HF, B3LYP, MP2, and (14,13) CASSCF levels, the values of  $\beta$  are orders of magnitude smaller than those predicted by semiempirical methods.

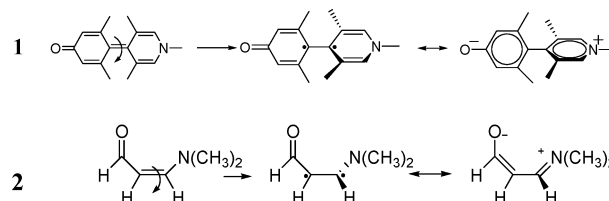
## Introduction

Chromophores with large hyperpolarizabilities,  $\beta$ , are valuable as components of photonic devices.<sup>1</sup> Theoretical computation of  $\beta$  has guided the design of new nonlinear optical systems; however, accurate calculation of the  $\beta$  at the ab initio level is computationally expensive for moderate-size chromophores. Large basis sets including diffuse functions and the inclusion of electron correlation are both important;<sup>2</sup> Bishop and co-workers have also shown that vibrational effects contribute to the nonlinear response.<sup>3</sup> Density functional theory (DFT) is a correlated method that is much faster than the ab initio second-order Møller–Plesset (MP2) or the coupled cluster singles and doubles (CCSD) method. While good agreement with experimental and other theoretical methods exists,<sup>4</sup> recent work suggests that DFT fails to treat charge transfer<sup>5</sup> and response properties<sup>6</sup> correctly in extended systems.

Tictoid (twisted intramolecular charge transfer) structures<sup>7</sup> have received much attention from Marks and Ratner<sup>8</sup> as a new class of promising nonlinear optical chromophores having tunable optical properties through a dihedral twist around a conjugating double bond. Highly twisted tictoid structures, recently synthesized by Marks and co-workers,<sup>9</sup> have both quinoidal and charge separated aromatic resonance forms, and are claimed to be zwitterionic at the 90° twist angle where there is no interring conjugation. Marks, Ratner, Brédas, and co-workers calculated an extremely large negative hyperpolarizability ( $\beta_{\mu\text{max}} = -3091 \times 10^{-30}$  esu) for a twisted tictoid merocyanine dye, 3,4-dimethyl-2',6'-dimethyl-4-quinopyran, **1** (Chart 1), using the sum-over-states MRD-CI/INDO/S semiempirical level of theory.<sup>10</sup> Previous semiempirical calculations by Albert et al. of other twisted  $\pi$ -chromophores<sup>11</sup> have also shown a large nonlinear optical (NLO) response. We attempted to compare the  $\beta$  calculated with semiempirical and ab initio methods but were thwarted; the B3LYP/6-31G\*\* method used by Marks, Ratner, and Brédas to optimize **1** yielded a wave function unstable to single excitations at 90°, indicating open-shell character instead of the proposed zwitterion.

In the present paper, we seek to more fully understand this tictoid system and, in addition, use a substituted twisted ethylene as a smaller analogue to test our computational methods. The

CHART 1: Twisted Chromophores **1** (tictoid)<sup>a</sup> and **2** (ethylenic)



<sup>a</sup> The diradical and zwitterion tictoid are not formal resonance structures at a pseudo- $C_{2v}$  90° twist angle because the covalent and ionic forms are of different symmetry.

smaller system will be quite different as it is nonaromatic, but higher level methods can be used to provide benchmarks for the larger system. Using both single-determinant and multiconfigurational ab initio methods, we calculate the dipole moment  $\mu$ , linear polarizability  $\alpha$ , and hyperpolarizability  $\beta$  for twisted double bonds at multiple levels of theory.

Accurately describing the delicate balance between zwitterionic and diradical singlet electronic states in a bond-breaking process has long frustrated many quantum chemists.<sup>12</sup> Ethylene, C<sub>2</sub>H<sub>4</sub>, is the simplest molecule with a  $\pi$ -bond that can be broken by rotating CH<sub>2</sub> groups with respect to one another.<sup>13</sup> The interplay among the three configurations that can be formed in a minimum basis set with two electrons in the  $\pi$  space of twisted ethylene and other polyenes, and the corresponding dramatic changes in dipole moment and polarization, has been studied previously.<sup>14</sup> In both the singly and doubly excited  $\pi \rightarrow \pi^*$  states, energy decreases as ethylene is twisted to 90°, while the covalent-diradical ground state increases in energy with twist angle. Any perturbation that breaks the symmetry will cause the excited states to mix giving rise to two zwitterion states. The energy gap between the singlet diradical and the excited state zwitterion is greatly decreased by donor and acceptor substituents,<sup>12a,15</sup> which also weaken the  $\pi$  bond due to the captodative effect.<sup>16</sup> Since breaking the symmetry of ethylene with unsymmetrical substitution allows the zwitterion and ground state to mix, Salem speculated that strong enough donor and acceptor substituents and/or a polar solvent will favor the zwitterion at some angles. System **1** no doubt has diradical and zwitterion ground states that grow closer in energy, leading to the increasing optical response with increasing twist angle.

\* Address correspondence to this author. E-mail: robinson@chem.washington.edu.

Multiconfigurational methods, such as the complete active space self-consistent field (CASSCF) method, are required to properly describe the singlet diradical.<sup>17</sup> A single Slater determinant method, such as Hartree–Fock (HF) or DFT, does not allow for partial occupation of molecular orbitals, and therefore often cannot accurately represent the degeneracies of a singlet diradical. A closed shell zwitterion is expected to require only a single determinant method. However, the CASSCF method requires a somewhat arbitrary choice of active space, i.e., of the “important” orbitals in the bond breaking reaction. For any double bond breaking by internal rotation, at least the  $\pi$  and  $\pi^*$  orbitals must be included. With the two electrons involved in the breaking bond, this results in a (2,2) CASSCF wave function (the first number designates electrons, the second active orbitals). For bond switching as shown in Chart 1, all the  $\pi$ -bonds involved in the switching may need to be included in the CAS active space. Since the number of CASSCF configurations increases factorially with active space size (the number of Slater determinants for a (12,12) CASSCF calculation is 3 867 864), the calculation can become prohibitively expensive. Additional electron correlation outside of the active space can be recovered by CASPT2<sup>18</sup> with many-body perturbation theory in conjunction with a CASSCF reference wave function.

For the electronic response properties, we use the Taylor series convention for the expansion of the dipole moment  $\mu$  in the presence of an electric field  $F$  at a fixed geometry:

$$\frac{-\partial E}{\partial F_i} = \mu_i = \mu_i^0 + \sum_j \alpha_{ij}^0 F_j + \frac{1}{2} \sum_{j,k} \beta_{ijk}^0 F_j F_k + \dots \quad (1)$$

The static polarizabilities can be written as derivatives of the dipole moment with respect to the field:

$$\alpha_{ij}^0 = \left. \frac{\partial \mu_i}{\partial F_j} \right|_{F=0} \quad (2)$$

$$\beta_{ijk}^0 = \left. \frac{\partial^2 \mu_i}{\partial F_k \partial F_j} \right|_{F=0} \quad (3)$$

The two-level perturbation theory expression for the linear polarizability and hyperpolarizability<sup>19</sup> is often used to qualitatively rationalize the response in terms of the difference between the ground (g) and the lowest optically allowed singly excited state (n) dipole moments  $\Delta\mu_{gn} = \mu_n - \mu_g = \langle \Psi_n | \hat{\mu} | \Psi_n \rangle - \langle \Psi_g | \hat{\mu} | \Psi_g \rangle$ , the transition dipole moment matrix element connecting the ground and excited state  $\mu_{gn} = \langle \Psi_g | \hat{\mu} | \Psi_n \rangle$ , and the energy difference between the two states  $E_{gn} = E_n - E_g$ :

$$\alpha \propto \frac{\mu_{gn}^2}{E_{gn}} \quad (4)$$

$$\beta_\mu \propto \frac{\Delta\mu_{gn} \mu_{gn}^2}{E_{gn}^2} \quad (5)$$

According to this simplified two-level model, the sign of  $\beta$  is determined completely by the difference in dipole moments in the ground and excited states in the direction of the original ground-state positive dipole. Most organic molecules have an excited state that is more charge separated than the ground state, and so will have a larger dipole moment than the ground state, giving a positive  $\beta$ . A more charge-separated ground state affords a negative  $\beta$ . The allowed singly excited state that

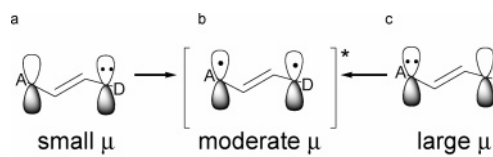


**Figure 1.** (a) The typical donor–acceptor chromophore under the influence of an electric field transfers charge in the opposite direction of the dipole moment, yielding a positive  $\beta$ , while a zwitterionic chromophore of type (c) transfers charge along the dipole moment, giving a negative  $\beta$ . A single excitation from a molecule of type (a) or type (c) yields an excited state with an intermediate dipole moment (b).

dominates the two-level model is often described as a simple transfer of an electron from the HOMO to the LUMO. In neutral donor–acceptor chromophores, the HOMO usually has greater coefficients on the donor group and the LUMO on the acceptor. For a neutral system (Figure 1a) a single electron excitation results in a larger dipole moment in the excited state (Figure 1b), and thus a positive  $\beta$ . In a zwitterion (Figure 1c), the most electronegative atom holds the formal negative charge defining the HOMO. Thus, in the excited state (Figure 1b), the more electronegative atom loses charge and the molecular dipole moment decreases with respect to the zwitterionic ground state, resulting in a negative  $\beta$ .

In a typical donor–acceptor chromophore with positive  $\beta$ , the donor is less electronegative than the acceptor, therefore the dipole moment vector is toward the donor, and the direction of easier charge movement, from donor to acceptor, causes an asymmetry in charge transfer that is anti-aligned with the dipole moment vector. A negative  $\beta$  is the result of easier charge movement through the  $\pi$  system in the same direction as the dipole moment. This occurs when electron density is located on the more electronegative group, as in charge-separated zwitterionics, when the typical “acceptor” group now contains more electron density and so becomes the donor group. The transfer of charge yields an overall smaller dipole moment as charge is moved from the more electronegative group to the more electropositive group. Thus, for a twisted asymmetric double bond, a sign change in  $\beta$  would be expected with increasing twist angle if the system switches from a neutral to a zwitterionic ground state ( $\beta$  would be zero for a symmetric olefin such as ethylene). With no asymmetry in the direction of charge movement,  $\beta$  is zero, as is seen for centrosymmetric systems.

## Computational Details

The Gaussian03<sup>20</sup> and MOLCAS<sup>21</sup> program suites were used for all calculations. Because Marks, Ratner, and co-workers used B3LYP<sup>22</sup> with the Pople 6-31G\*\* basis set for the geometry optimization of **1** (semiempirical methods were used to compute the optical properties), we chose the same optimization method for all systems to facilitate comparison. Twist angle geometries were enforced by constraining the two cis dihedral angles of the double bond. The optimized cisoid geometry for **2** is used for 0°. All optimizations were done without symmetry constraints. The B3LYP wave function for **1** did not converge at small twist angles due to steric interactions of the methyl groups ortho to the ring-connecting bond. Single point calculations converged the root-mean-square density matrix to 10<sup>−8</sup> and the energy to 10<sup>−6</sup> atomic units and DFT single point calculations used an ultrafine numerical integration grid [a pruned (99 590) grid]. The (2,2) CASSCF calculations included the  $\pi$  and  $\pi^*$  orbitals of the twisted bond in the active space, while larger CASSCF calculations included the entire bonding and anti-

bonding  $\pi$  system, including the donor and acceptor groups. The Hartree–Fock wave function for the planar optimized system was used for the first CASSCF initial guess, and the CASSCF wave functions were used for successive starting wave functions as the system was gradually twisted. The active space orbitals were visualized and carefully monitored for consistency, and the initial guess orbitals for the applied field calculations were always those previously optimized without the field.

The response property vector and tensor values<sup>23</sup> calculated are the magnitude of the dipole moment,  $\mu$ , in Debye, the rotational average  $((1/3)\text{Tr}\alpha)$  of the polarizability  $\alpha$ , given in  $\text{\AA}^3$ , and the component of the hyperpolarizability along the dipole, which is sometimes designated as  $\beta_\mu$  or  $\beta_{\text{vec}}$ , which we give in electrostatic units, is represented as

$$\beta_\mu = \frac{\sum_{i=x,y,z} \beta_i \mu_i}{|\mu|} \quad (6)$$

$$\beta_i = \frac{1}{3} \sum_{k=x,y,z} (\beta_{ikk} + \beta_{kik} + \beta_{kki}) \quad (7)$$

Kleinman symmetry<sup>24</sup> (independence of the order of differentiation) was enforced, so that terms differing only by a permutation of indices are assumed to be equal, i.e.,  $\beta_{xyy} = \beta_{yyx} = \beta_{yxy}$ .

Analytic derivatives were available for the HF method, via a coupled perturbed HF calculation, while numerical derivatives were used for MP2 and DFT to obtain the hyperpolarizability. At the CASSCF level, the finite difference numerical derivative technique determined elements of the polarizability and hyperpolarizability tensors:

$$\alpha_{ij} = \frac{\mu_i(F_j) - \mu_i(-F_j)}{2F_j} \quad (8)$$

$$\beta_{ijj} = \frac{\mu_i(F_j) + \mu_i(-F_j) - 2\mu_i(F=0)}{F_j^2} \quad (9)$$

An external electric field was created with two opposite point charges of 500e at 1000 Bohr on either side of the molecule along the  $x$ ,  $y$ , and  $z$  axes to create an electric field strength of 0.001 atomic units. From the multipole expansion, the use of opposite point charges creates a nonuniformity of the electric field in the region of the molecule that scales as (size of molecule/distance between charges)<sup>2</sup>. Assuming a molecule size of roughly 10 bohr, and the charges 1000 bohr apart, the nonuniformity of the field is  $(10/1000)^2$ , or  $10^{-4}$ . This is quite adequate for these calculations that do not take into account the effects of vibrational motion, solvent effects, or the field frequency. The large point charges would cause dramatic effects in the dipole of the system if the basis functions were not negligible at this distance.

## Results and Discussion

A stable 90° B3LYP/6-31G\*\* wave function, a CASSCF HOMO occupation number greater than 1.9 electrons for all twist angles, and an increasing dipole with increasing twist angle all indicate a closed shell, zwitterionic wave function for **2** at large twist angles. The electronic state of **1**, however, needs the entire  $\pi$ -system included in the CASSCF active space to be represented accurately. While **1** gives an unstable B3LYP/6-31G\*\* wave function at 90°, both MP2 and (2,2) CASSCF show an increasing dipole moment with increasing twist. The

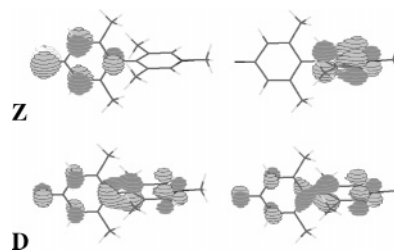


**Figure 2.** (14,13) CASSCF zwitterion (**Z**, top) and diradical (**D**, bottom) HOMO (left) and LUMO (right) for **1** at 90°.

**TABLE 1: Selected Geometric (B3LYP/6-31G\*\*) Data for Twisted  $\pi$ -Chromophores**

twist angle (deg)	central C–C (Å)		C–O (Å)		$\Delta r$ (Å) <sup>a</sup>	
	<b>1</b>	<b>2</b>	<b>1</b>	<b>2</b>	I–O	I–N
0	n/a <sup>b</sup>	1.368	n/a <sup>b</sup>	1.226	n/a <sup>b</sup>	n/a <sup>b</sup>
20	n/a <sup>b</sup>	1.370	n/a <sup>b</sup>	1.226	n/a <sup>b</sup>	n/a <sup>b</sup>
40	1.430	1.379	1.244	1.227	0.093	0.092
60	1.445	1.397	1.247	1.229	0.083	0.076
80	1.467	1.419	1.250	1.234	0.077	0.064
90	1.478	1.423	1.252	1.236	0.073	0.062

<sup>a</sup>  $\Delta r$  is the difference between the longest and shortest C–C bond in the two tictoid rings (O and N). <sup>b</sup> No convergence at small twist angles in **1** due to steric repulsion between methyl groups.

(14,13) CASSCF calculation that includes all switching  $\pi$  bonds gives a diradical wave function for the 90° twisted rings. However, the zwitterions and diradical states are very close in energy: a zwitterionic (14,13) CASSCF wave function for **1** was also found at 4.3 kcal/mol above the diradical wave function at 90°. The HOMO and LUMO for the diradical and zwitterionic 90° wave function for **1** are shown in Figure 2.

While the central carbon–carbon bond distances in **1** and **2** increase with twist angle (Table 1), they never approach a standard carbon–carbon single bond length of 1.5 Å. The oxygen–carbon bond lengths also slightly increase with twist angle for **1** and **2**, in accordance with an increasing contribution from the charge separated resonance form. One of the rationales given<sup>11a</sup> for assuming zwitterionic tictoid structures at 90° is the aromatic driving force associated with the charge separated species. Aromatic stabilization of **1** would no doubt make the charge separated form a large contributor in **1** even at small twist angles, resulting in the long central C–C and O–C bonds compared to **2** as seen at 40°. We estimated the aromatic character by the geometric criteria of bond length equalization. The maximum difference in carbon–carbon bond lengths,  $\Delta r$ , in the rings of **1** decreases with larger twist angles, but the pyridinium and oxygen substituted ring 90° values of  $\Delta r = 0.062$  and 0.073 for **1** are close to twice that of the  $\Delta r = 0.036$  of prototypical donor–acceptor ring chromophore *p*-nitroaniline calculated at the same level of theory. However, the delocalization, even if not complete, in each tictoid ring may stabilize the spin, making the diradical the ground-state wave function in **1**, but not **2**.

**Response Properties for 2.** While all methods show a peak in  $\alpha$  between the 60° and 90° twist angles for **2**, the CASSCF peaks are much larger (Figure 3). The CASSCF  $\beta$  values are quite different from those calculated at HF, B3LYP, or MP2, and so are plotted on a separate scale (Figure 5). The single determinant methods give a positive  $\beta$  (nitrogen acting as donor) at small twist angles, and then gradually shift to a negative  $\beta$  (oxygen acting as donor) at larger twist angles. At 90° there is minimal p-orbital overlap at the center twisting C–C bond, leading to a decrease in  $\beta$ , which is not as apparent with B3LYP. Calculations at the coupled-cluster singles and doubles/6-

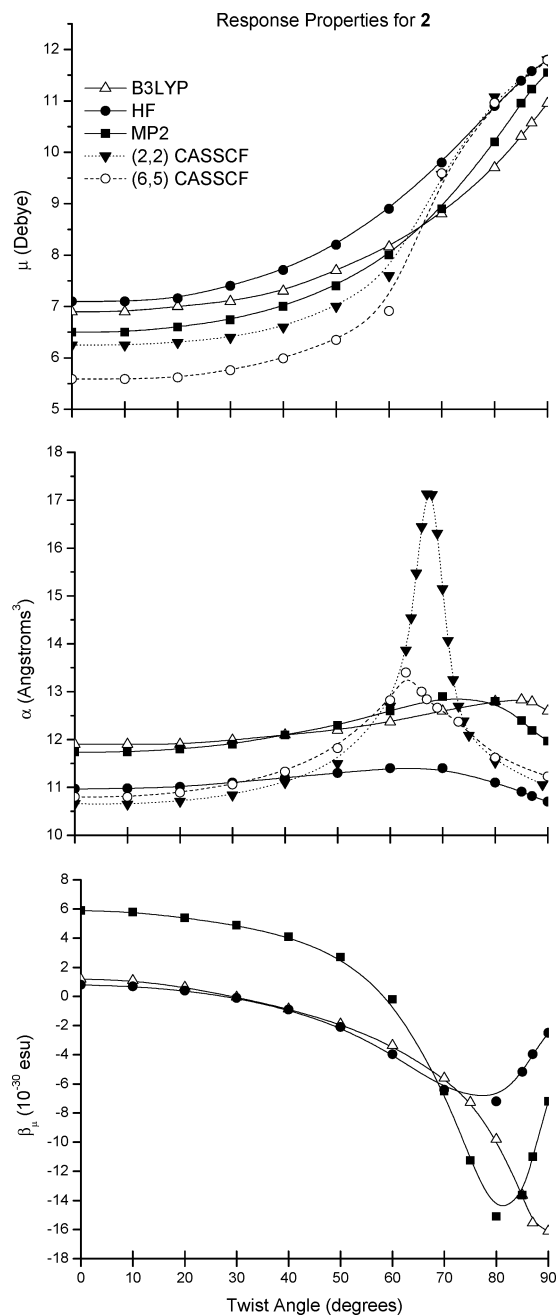


**Figure 3.** Dipole moments (top), linear polarizabilities (middle), and hyperpolarizabilities (bottom) for 2 calculated with 6-31+G\*\*.

31+G\*\* level with use of all  $\pi$ -electrons for excitations gave results remarkably similar to those of MP2/6-31+G\*\* for all properties. In contrast to these single determinant methods, the CASSCF results change suddenly between 65° and 70°, with large positive  $\beta$  on the lower twist angle and large negative  $\beta$  at the higher twist angle. The large CASSCF HOMO occupation number of 1.9 is linked to a large coefficient for the HF single determinant configuration. The extent to which CASSCF and HF disagree is therefore somewhat surprising. All methods show a smooth plot of the energies as a function of twist angle (Figure 4). For both 6-31G\* and 6-31+G\*\* basis sets, which are in impressive agreement for all methods, the linear polarizability peak corresponds to the zero of the hyperpolarizability as it goes from positive to negative. On the basis of this relation, and the fact that the diradical and zwitterionic states are very close in energy, we assume that the same state excitation is responsible for both  $\alpha$  and  $\beta$ . From Figure 5,  $\alpha$  and  $\beta$  appear to be

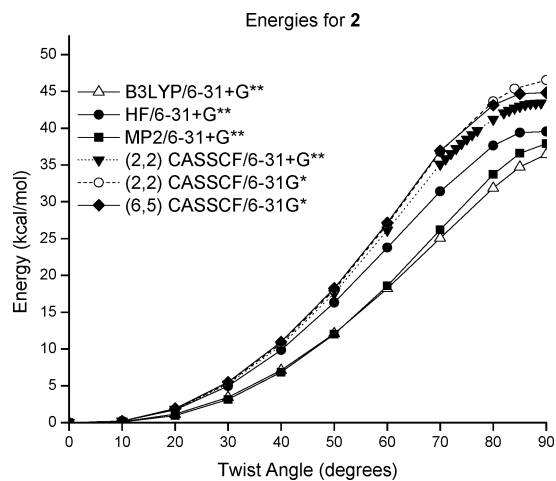


**Figure 4.** Energies for 2 as a function of twist angle.

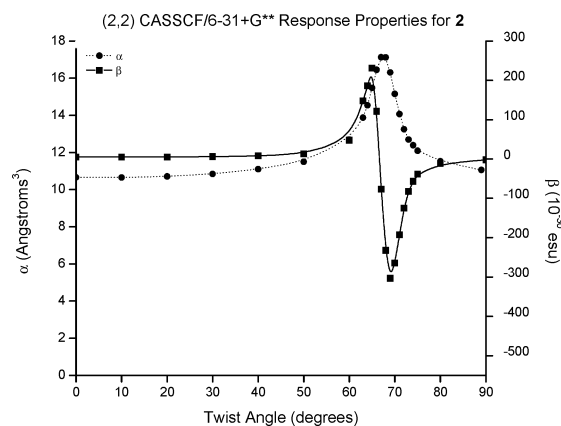


**Figure 5.** (2,2) CASSCF/6-31G\* linear polarizabilities and hyperpolarizabilities for 2.

derivatives with respect to twist angle rather than with respect to the field. A twisting bond or an applied field, however, would both cause an increase in the zwitterionic configuration. This similar effect is thus the cause for the successive derivative appearance of these properties. The relationship of  $\alpha$  and  $\beta$  can also be analyzed by combining the two-state model eqs 4 and 5 to give  $\beta_{\mu} \propto (\Delta\mu_{gn}/E_{gn})\alpha$ . The differences between  $\beta$  and  $\alpha$  are seen to be due to a change in sign of  $\Delta\mu_{gn}$  as explained in Figure 1, and a decreasing energy gap between the ground state  $g$  and excited state  $n$ .

As shown in Figure 1, a sign change in  $\beta$  represents a switch from a neutral to a zwitterionic ground state. A plot of (2,2) CASSCF “LUMO” occupation numbers in Figure 6 (this is more clearly depicted than in the (6,5) CASSCF occupation numbers in which five orbitals are partially occupied instead of two) shows a steeply changing occupation between 60° and 80°. The  $\beta_{xxx}$  tensor component dominates the total  $\beta$  value (the  $x$  contribution is also the dominant component of the dipole moment vector), and examining the LUMO occupation numbers with an applied field in the plus and minus  $x$  direction provides the rationale for the suddenly changing  $\beta$ . A plot of occupation numbers in this steeply changing region is shown in Figure 7, along with the occupation numbers for the system with a field applied in the  $\pm x$  directions. While it may not be obvious from Figure 7 that the difference in occupation numbers is responsible for 2’s large CASSCF positive and negative  $\beta$  peaks, Figure 8 shows a plot of these differences in the form of the second derivative of LUMO occupation number with respect to an applied field in the  $x$ -direction. The second configuration that is represented by these occupation numbers has a very large



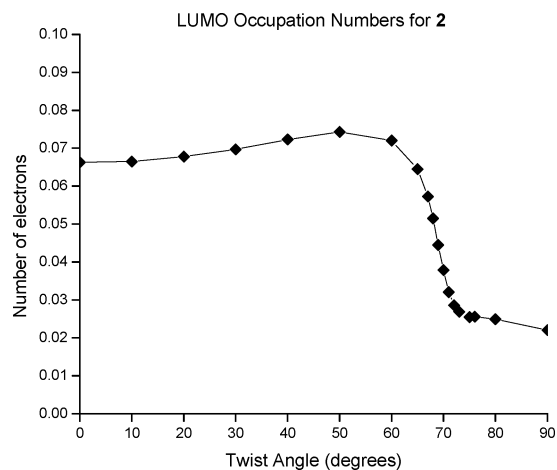


**Figure 6.** (2,2) CASSCF/6-31G\* LUMO occupation numbers for **2**.

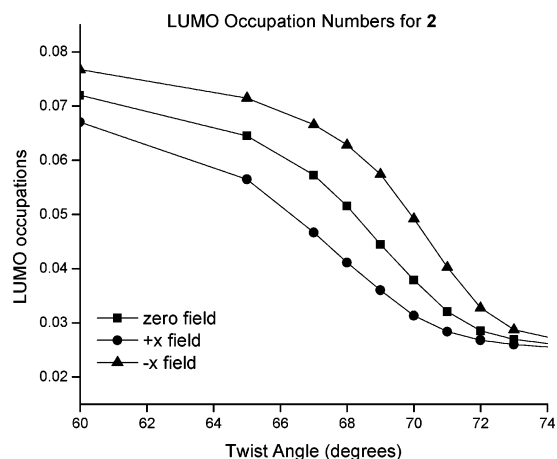


**Figure 7.** (2,2) CASSCF/6-31G\* LUMO occupation numbers for **2**, with no field (as shown in the figure above) and a field applied in the  $x$  and  $-x$  directions.

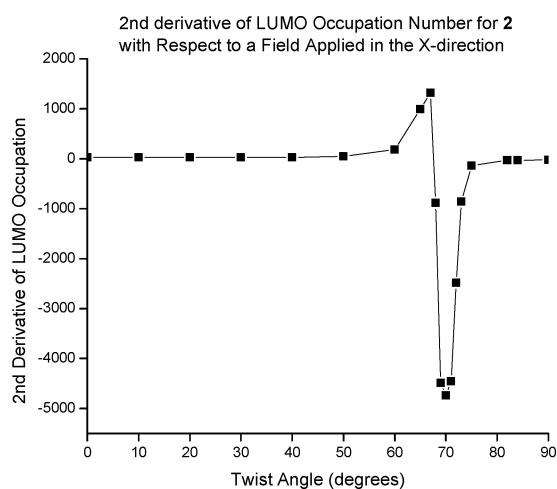


**Figure 8.** The second derivative of the (2,2) CASSCF/6-31G\* LUMO occupation numbers for **2** with respect to an applied field in the  $x$  direction. The plotted values are the (zero field + positive  $x$  field) + (zero field - negative  $x$  field) occupation numbers divided by the field strength<sup>2</sup>, which is analogous to the  $\beta$  derivative in eq 9.

second derivative. The positive values indicate that the field applied in the positive  $x$  direction causes a greater change than a field applied in the negative  $x$  direction, while the negative values indicate the opposite. Positive values correspond to a positive  $\beta$ , negative values to a negative  $\beta$ . Since an applied field would interact with the molecular dipole, which is

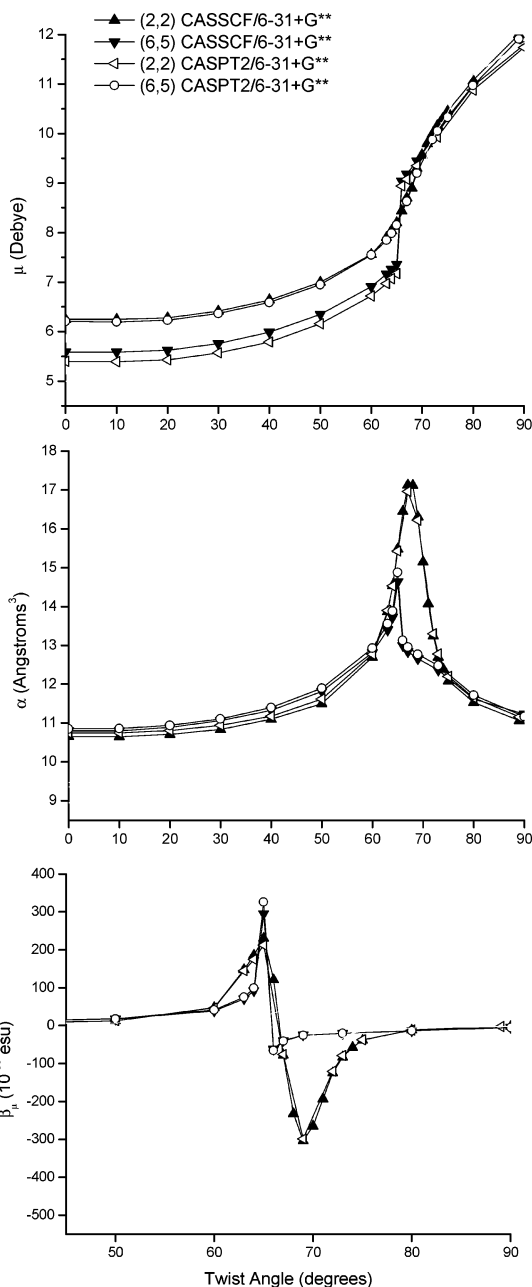


**Figure 9.** CASSCF and CASPT2/6-31+G\*\* dipole moments (top), linear polarizabilities (middle), and hyperpolarizabilities (bottom) for **2**.

intrinsically linked to the twist angle, the electric field response is also linked to the twist angle. At geometries between  $60^\circ$  and  $70^\circ$ , an applied field *along* the dipole moment (associated with a greater twist angle) would cause a much greater change in the electronic structure—to smaller LUMO occupation number—than an applied field antiparallel to the dipole. The opposite is true between  $70^\circ$  and  $80^\circ$  twist angles: an electric field *antiparallel* with the dipole moment leads the system to increasing LUMO occupation number. This opposing asymmetry, which is only possible in a method with partial occupation numbers given by the presence of another configuration, gives rise to the large positive and negative CASSCF  $\beta$  values for **2**. The CASSCF occupation numbers are quite sensitive to an applied field, causing the drastic sign changes in  $\beta$ .

Because **2** is small, we were able to include nondynamic electron correlation in the CAS active space via the CASPT2 method. Also included with the B3LYP/6-31G\*\* optimized

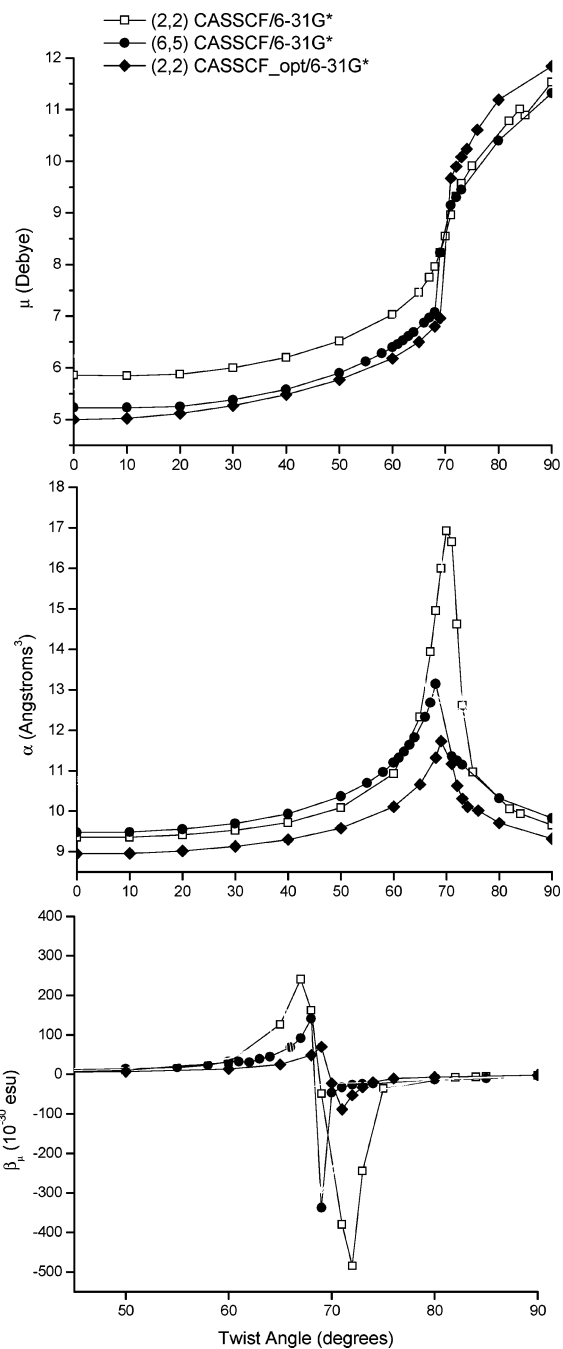


**Figure 10.** CASSCF/6-31G\* dipole moments (top), linear polarizabilities (middle), and hyperpolarizabilities (bottom) for **2**. The label CASSCF\_opt indicates **2** was optimized at the CASSCF/6-31G\* level, instead of at B3LYP/6-31G\*.

**TABLE 2: CAS Dipole Moments (Debye) for 2**

method	twist angle (deg)			
	0	20	40	60
(2,2) CASSCF/6-31G*	5.9	5.9	6.2	7.0
(2,2) CASSCF/6-31+G**	6.3	6.3	6.6	7.6
(2,2) CASPT2/6-31+G**	6.2	6.2	6.6	7.6
(6,5) CASSCF/6-31G*	5.2	5.3	5.6	6.4
(6,5) CASSCF/6-31+G**	5.6	5.6	6.0	6.9
(6,5) CASPT2/6-31+G**	5.4	5.4	5.8	6.7
(2,2) CASSCF_opt/6-31G* <sup>a</sup>	5.0	5.1	5.5	6.2

<sup>a</sup> This system was optimized at the (2,2) CASSCF/6-31G\* level instead of at the B3LYP/6-31G\* level.

geometry results are those at the CASSCF optimized geometry. These results are shown in Figures 9 and 10. At the MCSCF

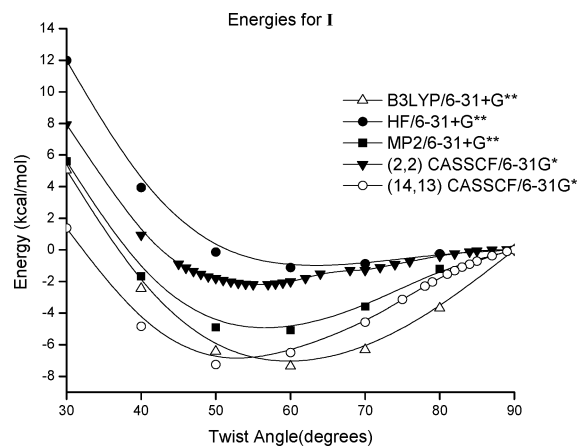


**Figure 11.** Energies for **1** as a function of twist angle.

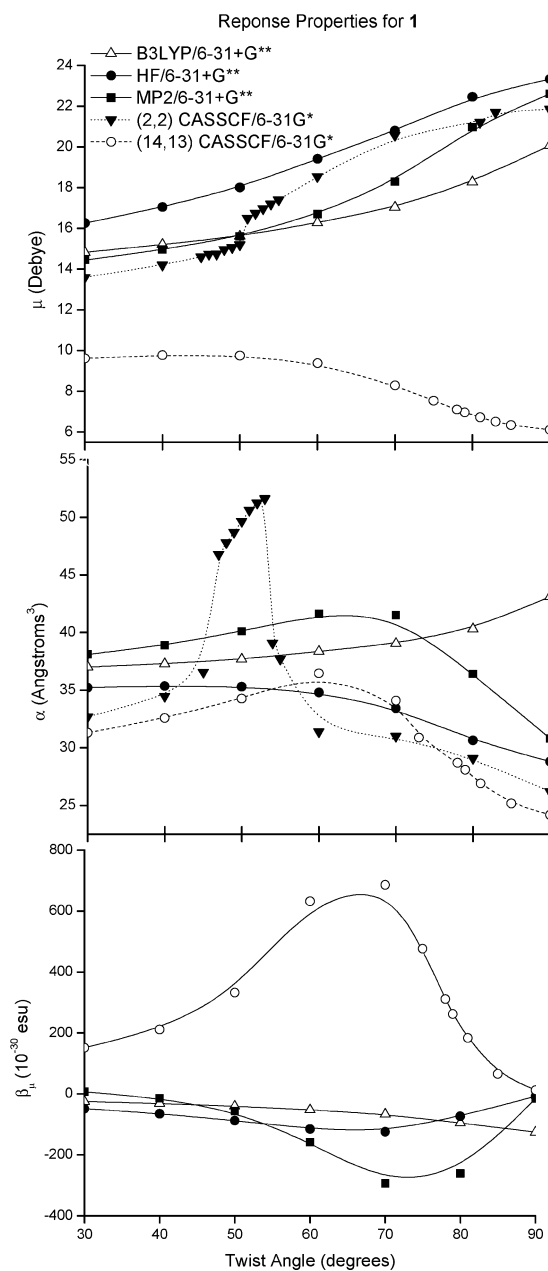


**Figure 12.** Dipoles (top), linear polarizabilities (middle), and hyperpolarizabilities (bottom) for **1**.

level of theory, the shape of the relation between  $\mu$  and twist angle appears insensitive to choice of active space, basis set, or

the inclusion of dynamic electron correlation (CASPT2 vs CASSCF). There is also little difference between the CAS results for B3LYP or CASSCF optimized geometries (designated as CASSCF\_opt in the plots). The magnitude of the dipole moment is dominated more by the size of the active space than by the basis set or electron correlation, as shown for twist angles between  $0^\circ$  and  $60^\circ$  in Table 2. For both the (2,2) and (6,5) CAS active space, the dipole magnitude is in the order CASSCF/6-31+G\*\* > CASPT2/6-31+G\*\* > CASSCF/6-31G\*. Both  $\alpha$  and  $\beta$  show that the turning point twist angle is determined by the basis set, but the shape of the peak is more dependent on active space. These results highlight the importance of fully treating the substituents in the active space. The dependence on active space illustrates the difficulty of using CASSCF because the choice of active space is subjective. Because the CASSCF optimized geometry, larger basis set, and CASPT2 results parallel those of CASSCF/6-31G\*\*/B3LYP/6-31G\*\*, we feel that results at the CASSCF/6-31G\*\*/B3LYP/6-31G\*\* level for the larger **1**, albeit the aromatic character of **1** makes it quite different from **2**, should provide a reasonable representation of the electronic properties.

**Response Properties for 1.** The energies for the analogous tictoid system, **1**, are shown in Figure 11. It has single determinant wave function  $\beta$  curves (Figure 12) similar to **2**. The shapes of the MP2 and HF curves are similar to the semiempirical results,<sup>10</sup> but 1–2 orders of magnitude smaller than the MRD-CI/INDO calculated  $\beta_{\max} = -3091 \times 10^{-30}$  esu. As mentioned, **1** has very different wave functions for the two CASSCF active spaces. A (2,2) CASSCF calculation predicts a zwitterionic structure (HOMO occupation number of 2.0 at  $90^\circ$ ). The (14,13) CASSCF calculation predicts a diradical (HOMO occupation number of 1.0 at  $90^\circ$ ). The (2,2) CASSCF calculation gives a large  $\alpha$  that is sharply peaked (Figure 12), and asymptotically large  $\beta$  values not shown on the graph for clarity (they are an order of magnitude larger than the plotted values:  $\beta = 3700 \times 10^{-30}$  esu at  $49^\circ$  and  $-5000 \times 10^{-30}$  esu at  $53^\circ$ ). This suggests an inherent instability in the CAS method when too small of an active space is used.

## Conclusions

In studying substituted twisted double bonds of varying degrees of diradical character, we find that the ab initio linear and nonlinear optical properties are very dependent on the choice of method. The choice of active space dominates the CASSCF response more than the basis set or the addition of dynamic electron correlation. The donor and acceptor tictoid, **1**, is a ground state diradical, but this is seen only with (14,13) CASSCF. The (2,2) CASSCF values give numerically unstable values for  $\beta$ , varying over an order of magnitude within  $2^\circ$  of twist. It is thus very important to include the entire  $\pi$ -system in the CASSCF active space to accurately represent the ground state diradical character of this important class of twisted chromophore. While the zwitterionic form would undoubtedly be stabilized in the condensed phase, the diradical nature of these systems in the gas phase has been largely ignored in the literature. Single-determinant ab initio methods (HF, B3LYP, and MP2) give a negative  $\beta$ , in agreement with previous semiempirical calculations on **1**,<sup>10</sup> but with values much smaller (by 1.5–2 orders of magnitude) than the analogous MRD-CI/INDO results.

The ethelnyic donor and acceptor system, **2**, is more zwitterionic. Even though this system appears to be closed shell, the multiconfigurational results do not agree with the single determinant methods. The CAS calculations may be numerically

unstable because of the large change in response properties over a few degrees of twist. It is difficult to determine whether a closed shell method such as Hartree–Fock, MP2, or B3LYP could not properly capture the response of the system to an applied field because of an inflexible wave function, or whether the CASSCF method is too sensitive to an applied field, allowing overly facile crossing between the diradical and zwitterionic states. According to Figure 5, **2** is predominantly closed shell, but exhibits significant differences from the closed shell methods as seen in Figures 3 and 4. The small amount of electron population in the LUMO (i.e., of the other state) is extremely sensitive to an applied field, perhaps unphysically so. The large change in the sign and magnitude of  $\beta$  obtained by multiconfigurational methods over very small ranges in the twist angle of **2** (Figure 6) is similar to those seen with too small of an active space for **1**, and is probably more indicative of numerical instabilities with the application of a field than actual hyperpolarizabilities. In neither system do we take into account the effect of vibrations on the hyperpolarizability. The electronic hyperpolarizability is very sensitive to geometry, and the vibrational contribution to the hyperpolarizability (both from zero-point energy and nuclear vibrational motion) is expected to be large. Measured values would likely differ greatly from computed electronic contributions because of these vibrational effects, the sensitivity to method, and the large changes expected in condensed phases.

The delicate balance between the diradical and zwitterionic forms is the primary factor in determining the response for these systems at all levels of theory. It is this electronic balance that allows the two forms to transfer charge preferentially in one direction, creating the asymmetry required for a nonlinear response. This work underscores the fact that this potentially important archetype remains a great challenge to the theoretical community.

**Acknowledgment.** We thank AFOSR and NSF's STC-MDITR (DMR-0120967) for financial support of this research. C.M.I. would like to thank Todd Markle, William Karney, and John Goddard for helpful discussions of BS-UDFT calculations, Kiril Tsemekhman for inspirational conversations about DFT and computational methodologies, Bruce Eichinger for suggesting this project, and Bart Kahr for editing, Jean-Luc Brédas and Demétrio A. da Silva Filho for insights in regards to the semiempirical work. The authors also thank Dave Hrovat and Weston Thatcher Borden for computational support.

## References and Notes

- (1) (a) Dalton, L. *Adv. Polym. Sci.* **2002**, *158*, 1. (b) Zyzyk, M. G.; Dirk, C. W., Eds. *Characterization Techniques and Tabulations for Organic Nonlinear Optical Materials*; Marcel Dekker: New York, 1998. (c) Torrent-Sucarrat, M.; Solà, M.; Duran, M.; Luis, J. M.; Kirtman, B. *J. Chem. Phys.* **2003**, *118*, 711.
- (2) (a) Borden, W. T.; Davidson, E. R. *Acc. Chem. Res.* **1996**, *29*, 67. (b) Davidson, E. R.; Feller, D. *Chem. Rev.* **1986**, *86*, 681. (c) Kanis, D. R.; Ratner, M. A.; Marks, T. J. *Chem. Rev.* **1994**, *94*, 195. (d) Torrent-Sucarrat, M.; Solà, M.; Duran, M.; Luis, J. M.; Kirtman, B. *J. Chem. Phys.* **2004**, *120*, 6346 and references therein.
- (3) (a) Bishop, D. M. *Rev. Mod. Phys.* **1990**, *62*, 343. (b) Bishop, D. M.; Kirtman, B.; Kurtz, H. A.; Rice, J. E. *J. Chem. Phys.* **1993**, *98*, 8024 and references therein.
- (4) Liao, Y.; Eichinger, B. E.; Firestone, K. A.; Haller, M.; Luo, J.; Kaminsky, W.; Benedict, J. B.; Reid, P. J.; Jen, A. K.-Y.; Dalton, L. R.; Robinson, B. H. *J. Am. Chem. Soc.* **2005**, *127*, 2758.
- (5) (a) Dreuw, A.; Head-Gordon, M. *J. Am. Chem. Soc.* **2004**, *126*, 4007. (b) Dreuw, A.; Weisman, J. L.; Head-Gordon, M. *J. Chem. Phys.* **2003**, *119*, 2943.
- (6) (a) Tozer, D. J.; Handy, N. C. *J. Chem. Phys.* **1998**, *109*, 10180. (b) Tozer, D. J. *J. Chem. Phys.* **2003**, *119*, 12697. (c) van Faassen, M.; de Boeij, P. L.; van Leeuwen, R.; Berger, J. A.; Snijders, J. G. *Phys. Rev.*

- Lett.* **2002**, 88, 186401. (d) Champagne, B.; Perpète, E. A.; Jacquemin, D.; van Gisbergen, S. J. A.; Baerends, E.-J.; Soubra-Ghaoui, C.; Robins, K. A.; Kirtman, B. *J. Phys. Chem. A* **2000**, 104, 4755.
- (7) Grabowski, Z. R.; Rotkiewicz, K.; Rettig, W. *Chem. Rev.* **2003**, 103, 3899.
- (8) (a) Pati, S. K.; Marks, T. J.; Ratner, M. A. *J. Am. Chem. Soc.* **2001**, 123, 7287. (b) Facchetti, A.; Hutchison, G. R.; Keinan, S.; Ratner, M. A. *Inorg. Chim. Acta* **2004**, 357, 3980.
- (9) (a) Kang, H.; Facchetti, A.; Stern, C. L.; Rheingold, A. L.; Kassel, W. S.; Marks, T. J. *Org. Lett.* **2005**, 7, 3721. (b) Kang, H.; Facchetti, A.; Pei, Z.; Jiang, H.; Yang, Y.; Cariati, E.; Righetto, S.; Ugo, R.; Zuccaccia, C.; Macchioni, A.; Stern, C. L.; Liu, Z.; Ho, S.-T.; Marks, T. J. *Angew. Chem., Int. Ed.* **2005**, 44, 7922.
- (10) (a) Keinan, S.; Zojer, E.; Brédas, J.-L.; Ratner, M.; Marks, T. *THEOCHEM* **2003**, 633, 227. (b) Albert, I.; Marks, T.; Ratner, M. *J. Am. Chem. Soc.* **1998**, 120, 11174.
- (11) (a) Albert, I.; Marks, T.; Ratner, M. *J. Am. Chem. Soc.* **1997**, 119, 3155. (b) Albert, I.; Marks, T.; Ratner, M. *J. Phys. Chem.* **1996**, 100, 9714.
- (12) (a) Salem, L.; Leforestier, C.; Segal, G.; Wetmore, R. *J. Am. Chem. Soc.* **1975**, 97, 479. (b) Mulliken, R. S. *Phys. Rev.* **1932**, 41, 751.
- (13) (a) Moskowitz, J. W.; Harrison, M. C. *J. Chem. Phys.* **1965**, 42, 1726. (b) Kaldor, U.; Shavitt, I. *J. Chem. Phys.* **1968**, 48, 191. (c) Mulliken, R. S.; Roothaan, C. C. J. *Chem. Rev.* **1947**, 41, 219. (d) Buenker, R. J. *J. Chem. Phys.* **1968**, 48, 1368.
- (14) (a) Salem, L. *Acc. Chem. Res.* **1979**, 12, 87. (b) Viel, A.; Krawczyk, R.; Manthe, U.; Domcke, W. *Angew. Chem., Int. Ed.* **2003**, 42, 3434. (c) Wulfman, C. E.; Kumei, S. *Science* **1971**, 172, 1061. (d) Bonacic-Koutecky, V.; Bruckmann, P.; Hiberty, P.; Koutecky, J.; Leforestier, C.; Salem, L. *Angew. Chem., Int. Ed. Engl.* **1975**, 14, 575. (e) Brooks, B. R.; Schaefer, H. F., III. *J. Am. Chem. Soc.* **1979**, 101, 307.
- (15) Nagase, S.; Morokuma, K.; *J. Am. Chem. Soc.* **1978**, 100, 1661.
- (16) Viehe, H. G.; Janousek, Z.; Merenya, R. *Acc. Chem. Res.* **1985**, 18, 148.
- (17) (a) Davidson, E. R. *Int. J. Quantum Chem.* **1998**, 69, 241. (b) For an excellent review in navigating the Homeric journey of calculations on open-shell systems see: Bally, T.; Borden, W. T. *Reviews in Computational Chemistry*; Lipkowitz, K. B., Boyd, D. B., Eds.; John Wiley & Sons: New York, 1999; Vol. 13, pp 1–97.
- (18) (a) Andersson, K.; Malmqvist, P.-Å.; Roos, B. O.; Sadlej, A. J.; Wolsink, K. *J. Phys. Chem.* **1990**, 94, 5483. (b) Andersson, K.; Malmqvist, P.-Å.; Roos, B. O. *J. Chem. Phys.* **1992**, 96, 1218.
- (19) (a) Oudar, J. L. *J. Chem. Phys.* **1977**, 67, 446. (b) Brédas, J. L.; Meyers, F.; Pierce, B. M.; Zyss, J. *J. Am. Chem. Soc.* **1992**, 114, 4928.
- (20) Frisch, M. J.; Trucks, G. W.; Schlegel, H. B.; Scuseria, G. E.; Robb, M. A.; Cheeseman, J. R.; Montgomery, J. A., Jr.; Vreven, T.; Kudin, K. N.; Burant, J. C.; Millam, J. M.; Iyengar, S. S.; Tomasi, J.; Barone, V.; Mennucci, B.; Cossi, M.; Scalmani, G.; Rega, N.; Petersson, G. A.; Nakatsuji, H.; Hada, M.; Ehara, M.; Toyota, K.; Fukuda, R.; Hasegawa, J.; Ishida, M.; Nakajima, T.; Honda, Y.; Kitao, O.; Nakai, H.; Klene, M.; Li, X.; Knox, J. E.; Hratchian, H. P.; Cross, J. B.; Bakken, V.; Adamo, C.; Jaramillo, J.; Gomperts, R.; Stratmann, R. E.; Yazyev, O.; Austin, A. J.; Cammi, R.; Pomelli, C.; Ochterski, J. W.; Ayala, P. Y.; Morokuma, K.; Voth, G. A.; Salvador, P.; Dannenberg, J. J.; Zakrzewski, V. G.; Dapprich, S.; Daniels, A. D.; Strain, M. C.; Farkas, O.; Malick, D. K.; Rabuck, A. D.; Raghavachari, K.; Foresman, J. B.; Ortiz, J. V.; Cui, Q.; Baboul, A. G.; Clifford, S.; Cioslowski, J.; Stefanov, B. B.; Liu, G.; Liashenko, K.; Piskorz, P.; Komaromi, I.; Martin, R. L.; Fox, D. J.; Keith, T.; Al-Laham, M. A.; Peng, C. Y.; Nanayakkara, A.; Challacombe, M.; Gill, P. M. W.; Johnson, B.; Chen, W.; Wong, M. W.; Gonzalez, C.; and Pople, J. A.; *Gaussian 03*, Revision B.04; Gaussian, Inc.: Wallingford, CT, 2004.
- (21) Andersson, K.; Barysz, M.; Bernhardsson, A.; Blomberg, M. R. A.; Carissan, Y.; Cooper, D. L.; Fülcher, M. P.; Gagliardi, L.; de Graaf, C.; Hess, B. A.; Hagberg, D.; Karlström, G.; Lindh, R.; Malmqvist, P.-Å.; Nakajima, T.; Neogrády, P.; Olsen, J.; Raab, J.; Roos, B. O.; Ryde, U.; Schimmelpfennig, B.; Schütz, M.; Seijo, L.; Serrano-Andrés, L.; Siegbahn, P. E. M.; Ståhring, J.; Thorsteinsson, T.; Veryazov, V.; Widmark, P.-O. *MOLCAS*, version 5.4; Department of Theoretical Chemistry, Chemical Centre, University of Lund: P.O.B. 124, S-221 00 Lund, Sweden, 2002.
- (22) Becke's three-parameter hybrid functional: Becke, A. D. *J. Chem. Phys.* **1993**, 98, 5648. With the Lee–Yang–Parr correlation functional: Lee, C.; Yang, W.; Parr, R. G.; *Phys. Rev. B* **1988**, 37, 785.
- (23) Conversion factors from atomic units to the units used for the quantities of interest are the following: (i) 1 au of  $\mu \equiv ea_0 = 2.542 \times 10^{-18}$  statvolt cm<sup>2</sup> = 2.542 D; (ii) 1 au of  $\alpha \equiv e^2 a_0^2 E_h^{-1} = 1.482 \times 10^{-25}$  cm<sup>3</sup> = 0.1482 Å<sup>3</sup>; (iii) 1 au of  $\beta \equiv e^3 a_0^3 E_h^{-2} = 8.639 \times 10^{-33}$  statcoulomb<sup>-1</sup> cm<sup>5</sup> =  $8.639 \times 10^{-33}$  cm<sup>5</sup> esu<sup>-1</sup>. Note: In the literature, the hyperpolarizability unit esu is often used to mean cm<sup>5</sup> esu<sup>-1</sup>, and we will adopt this convention.
- (24) Kleinman, D. A. *Phys. Rev.* **1962**, 126, 1977.